

40-Hz Auditory Steady-State Responses in Schizophrenia: Toward a Mechanistic Biomarker for Circuit Dysfunctions and Early Detection and Diagnosis

Tineke Grent-'t-Jong, Marion Brickwedde, Christoph Metzner, and Peter J. Uhlhaas

ABSTRACT

There is converging evidence that 40-Hz auditory steady-state responses (ASSRs) are robustly impaired in schizophrenia and could constitute a potential biomarker for characterizing circuit dysfunctions as well as enable early detection and diagnosis. Here, we provide an overview of the mechanisms involved in 40-Hz ASSRs, drawing on computational, physiological, and pharmacological data with a focus on parameters modulating the balance between excitation and inhibition. We will then summarize findings from electro- and magnetoencephalographic studies in participants at clinical high risk for psychosis, patients with first-episode psychosis, and patients with schizophrenia to identify the pattern of deficits across illness stages, the relationship with clinical variables, and the prognostic potential. Finally, data on genetics and developmental modifications will be reviewed, highlighting the importance of late modifications of 40-Hz ASSRs during adolescence, which are closely related to the underlying changes in GABA (gamma-aminobutyric acid) interneurons. Together, our review suggests that 40-Hz ASSRs may constitute an informative electrophysiological approach to characterize circuit dysfunctions in psychosis that could be relevant for the development of mechanistic biomarkers.

<https://doi.org/10.1016/j.biopsych.2023.03.026>

The identification of noninvasive biomarkers for diagnosis and prognosis is a fundamental challenge in current schizophrenia (ScZ) research (1). Importantly, biomarkers should ideally allow insights into the underlying pathophysiological mechanisms and facilitate links to preclinical research (2). One potential candidate is the 40-Hz auditory steady-state response (ASSR). SSRs reflect stimulus rate-dependent, evoked activity to constant periodic stimuli in different sensory modalities that can be detected using electroencephalography (EEG) and magnetoencephalography (MEG). ASSRs show a peak frequency around 40-Hz in humans (3) in contrast to other sensory modalities, such as visual SSRs (4).

Kwon *et al.* (5) investigated 40-Hz ASSRs for the first time in patients with ScZ by using EEG, demonstrating reduced power and phase delay to 40-Hz stimulation. These findings provided further support for the hypothesis that neural circuits were compromised in ScZ to generate oscillations in the gamma band (30–100 Hz) (6). During normal brain functioning, gamma-band oscillations have been proposed to facilitate coordination of distributed neuronal activity to support the generation of perception and cognition (7) and are accordingly a candidate mechanism for the pervasive sensory and cognitive deficits in ScZ (8).

The initial findings by Kwon *et al.* (5) have been replicated by several groups using both EEG and MEG (9–11). In addition, more recent studies have examined 40-Hz ASSRs in

participants at clinical high risk for psychosis (CHR-P) and first-episode psychosis (FEP) patients (12,13), raising the possibility that 40-Hz ASSRs could be used for early detection and diagnosis of early-stage psychosis.

Despite the extensive evidence of 40-Hz ASSR deficits in ScZ, several questions remain regarding their significance and interpretation. Therefore, the goal of this article is to provide a state-of-the-art overview of 40-Hz ASSRs as a mechanistic biomarker for elucidating circuit dysfunctions in ScZ as well as for early detection and diagnosis. Accordingly, we will summarize the mechanisms underlying 40-Hz ASSRs, drawing on computational, physiological, and pharmacological perspectives. This will be followed by an overview of current studies in CHR-P participants, FEP groups, and patients with ScZ. Finally, evidence from genetics as well as recent studies on 22q11.2 deletion syndrome will be reviewed together with data on developmental modifications, followed by recommendations for future research.

GENERATORS UNDERLYING 40-HZ ASSRS IN HUMAN AND ANIMAL ELECTROPHYSIOLOGY

Current EEG and MEG studies interpret 40-Hz ASSRs as a probe for measuring the resonance frequency of auditory circuits. However, while initial findings focused on auditory regions as the main areas involved in the generation of the

40-Hz ASSR, in particular the medial Heschl's gyrus (14,15), more recent work has suggested that 40-Hz ASSRs involve a more extensive network.

Evidence for the contribution of frontal generators toward 40-Hz ASSRs in humans comes from MEG/EEG (16,17) as well as from intracranial recordings (18) (Figure 1). In addition, 40-Hz ASSRs have been observed in parietal areas (14) and in the inferior colliculus (19). Tada *et al.* (18) analyzed high-density electrocorticography in response to ASSRs at 20, 30, 40, 60, 80, 120, and 160 Hz using two common techniques to analyze steady-state activity, intertrial phase coherence (ITPC) (20) and spectral power estimates. The first refers to the consistency of phase angles across trials, therefore reflecting only evoked activity. The latter encompasses both evoked activity and induced components, of which the timing can differ between trials. Modulation of ITPC and spectral power was maximal at 40-Hz stimulation and was distributed across temporal, parietal, and frontal cortices.

In addition, there is evidence for a role of the thalamus, in particular the medial geniculate body, in the generation of 40-Hz ASSRs from MEG/EEG, positron emission tomography, and functional magnetic resonance imaging data (12,19,21). These findings were corroborated by a study showing that electrical stimulation of thalamic neurons evoked gamma-band activity around 40-Hz in the auditory cortex (22). Moreover, recent work has shown that generators extend to additional subcortical areas, including the hippocampus (12) and brainstem (15).

CIRCUIT MECHANISMS OF 40-HZ ASSRs: EXCITATION/INHIBITION BALANCE PARAMETERS

Unlike transient evoked potentials, SSRs require a high temporal resolution for coordinated signal integration as well as for transmission and processing, especially in higher-frequency ranges (23). Initial efforts focused on disclosing whether SSRs simply constitute a summation of event-related potentials or whether they reflect the entrainment of rhythmic oscillatory activity. While some studies supported to the

summation hypothesis (24,25), it is more likely that both models are nonexclusive and interacting to produce the ASSR response.

As such, it has been proposed that early transient components of the ASSR response may reflect event-related potential processes, while late-latency, sustained responses reflect rhythmic activity (11,16). This theory is supported by evidence indicating that ITPC is larger for the late sustained 40-Hz ASSRs (150–500 ms) compared with ITPC modulation between 0 and 50 ms (12,26), suggesting that sustained rhythmic activity may be only observed after the early evoked component. In this context, it is important to highlight that neural oscillations reflect synchronous, rhythmic activity of neuronal ensembles that occur in a circumscribed frequency range and is sustained over several cycles (27). Accordingly, neural oscillations need to be distinguished from broadband power changes, transient responses, and aperiodic activity (28), and recent methods have been introduced to separate these processes (29).

Gamma-band oscillations emerge from the balance between excitation and inhibition (E/I) in neural networks (30) (Figure 2). Specifically, the time constants of inhibitory post-synaptic potentials of GABAergic (gamma-aminobutyric acid-ergic) parvalbumin-positive (PV+) interneurons are ideally suited to generate 40-Hz rhythms (31). This has been shown, for instance, through hippocampal excitation of PV+ interneurons by means of NMDA receptors (NMDARs), which resulted in 40-Hz transient oscillatory responses in pyramidal cells (32,33).

PV+ interneurons mainly target the perisomatic region of pyramidal cells and can therefore control their output effectively as opposed to somatostatin-expressing interneurons that mainly inhibit the apical dendrite (34). Computational studies have further demonstrated that these anatomical and electrophysiological properties of PV+ interneurons are crucial for the generation of gamma-band oscillations and that several key E/I balance parameters determine their power and coherence (35). Moreover, the strength of exerted inhibition, which in turn is dependent on the strength of NMDAR activation as well

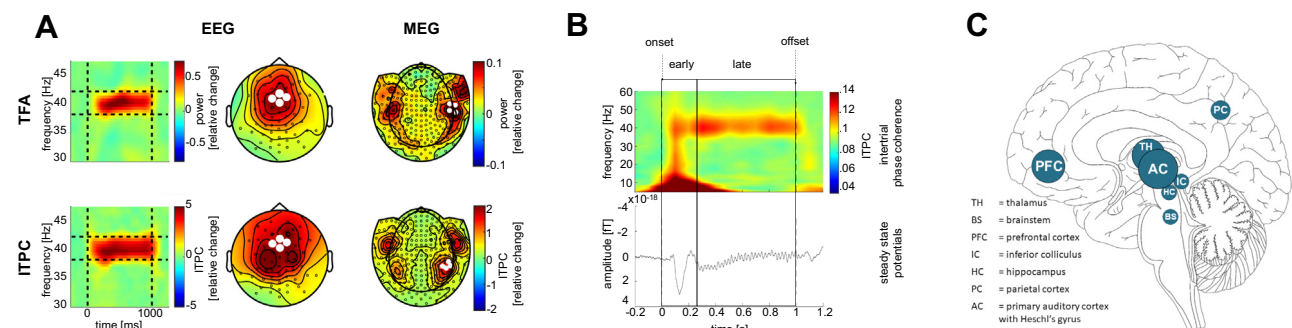


Figure 1. 40-Hz auditory steady-state responses (ASSRs) in electroencephalographic/magnetoencephalographic (EEG/MEG) data. **(A)** 40-Hz auditory stimulation elicits SSRs measurable with EEG/MEG. Illustrated are typical response patterns in both 40-Hz power (analyzed with time–frequency analysis [TFA]) and phase (analyzed with intertrial phase coherence [ITPC]). In EEG recordings, these responses can be observed over frontocentral regions, while in MEG they are localized over temporal regions. **(B)** 40-Hz ASSRs consist of early transient and late sustained activity: Illustrated are a typical neuronal ASSR of human recordings using MEG, depicted by ITPC values and the averaged steady-state potential. The difference between the early onset and the late sustained activity are clearly visible. **(C)** Overview of generators involved in 40-Hz ASSRs from multimodal imaging studies using positron emission tomography/functional magnetic resonance imaging/EEG/MEG and intracranial recordings. (From P.J. Uhlhaas, Ph.D., *et al.*, unpublished data, November 2022.)

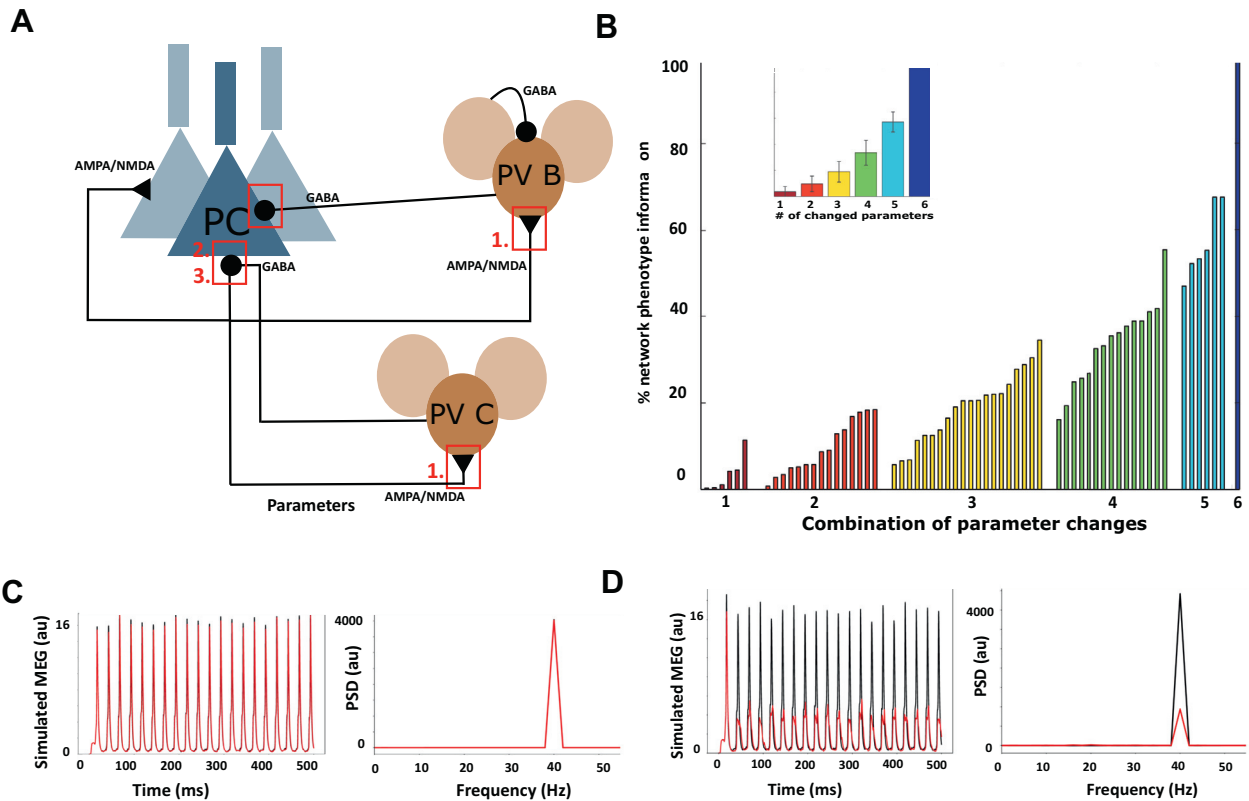


Figure 2. Excitation/inhibition balance mechanisms of 40-Hz auditory steady-state responses (ASSRs) and schizophrenia (ScZ)-associated microcircuit alterations. **(A)** 40-Hz ASSRs are generated through the interaction between populations of excitatory pyramidal cells (PCs) and parvalbumin (PV)-positive interneurons, which can be subdivided into two groups, basket cells (PV B) and chandelier cells (PV C). ScZ-associated changes mainly occur at NMDA receptors at PC-PV synapses (1.) and PV-PC synapses (2. and 3.). **(B)** Simulated circuit parameters and 40-Hz ASSR deficits in ScZ: 6 ScZ-associated network parameters (GABA [γ -aminobutyric acid] levels at PCs, GABA levels at inhibitory cells, number of inhibitory connections to PCs, number of inhibitory connections to inhibitory cells, prolonged GABAergic time constant at PCs, prolonged GABAergic time constant at inhibitory cells) were changed in a computational model and the network response to 40-Hz click trains was simulated. The panel shows the normalized mutual information between GABAergic network parameters and a 40-Hz ASSR power reduction (inset shows mean and standard deviation for the number of changed parameters), demonstrating that only a combination of several parameters, not single parameters, predicted 40-Hz ASSR power reductions. **(C, D)** Computational modeling of PV-interneuron subtypes and 40-Hz ASSRs in ScZ: chandelier cells at a realistic ratio (10% of PV interneurons) do not contribute significantly to the 40-Hz ASSR deficit. Basket cells are predominantly responsible for the power reduction (97). Simulated magnetoencephalography (MEG) signal (left) and resulting power spectral density (PSD) (right) for 40-Hz ASSR. The black curves represent the control model configuration and the red curves represent changes to the GABAergic system at chandelier cells associated with ScZ. **(D)** Simulated MEG signal (left) and resulting PSD (right) for 40-Hz ASSR. The black curves represent the control model configuration and the red curves represent changes to the GABAergic system at basket cells associated with ScZ. Only the basket cell changes are able to significantly reduce the 40-Hz ASSR power. [Modified with permission from Metzner *et al.* (37).]

as on the maximal conductance of the GABAergic synapses, also crucially influences 40-Hz ASSR power (36–39).

Further evidence for the role of E/I balance parameters in the generation of 40-Hz ASSRs comes from pharmacological studies. In human EEG recordings, the NMDAR antagonist ketamine has been associated with an increase in the power of the 40-Hz ASSRs (40). In contrast, administration of the NMDAR antagonist MK 801 into the medial geniculate body in mice was associated with reduced 40-Hz ASSRs in the auditory cortex, without affecting the early transient response (41). Such diverging findings could be explained by different locations and dosages of drug administration. For instance, Sivarao *et al.* (42) showed that NMDAR channel occupancy is related to the modulation of both power and phase locking of 40-Hz ASSRs, with lower ketamine dosages causing an increase

in spectral power and ITPC, while higher doses caused decreased 40-Hz ASSRs.

Similarly, there is emerging evidence that GABAergic neurotransmission modulates 40-Hz ASSRs. Increasing inhibition via administration of the GABA_A agonist muscimol results in increased power and phase locking of 40-Hz ASSRs in humans (43). Moreover, selective PV+ interneuron excitation using optogenetic stimulation in the basal forebrain in rats increased ASSR responses in the auditory cortex only when stimulating at 40 Hz but not at other frequencies (44). Accordingly, these data indicate that modulation of both power and ITPC values of 40-Hz ASSRs are a sensitive marker for E/I balance alterations that could allow the identification of circuit mechanisms in ScZ. In particular, both PV+ interneuron activation and the excitatory drive mediated through NMDARs have a mechanistic impact on 40-Hz ASSRs.

40-HZ ASSRs IN ScZ: PATTERN OF DEFICITS AND CORRELATIONS WITH CLINICAL VARIABLES

Approximately 40 studies have investigated 40-Hz ASSRs in patients with ScZ using both EEG and MEG [for a recent review, see (44)]. The large majority of studies have reported a reduction in both ITPC and power of 40-Hz ASSRs with medium-level effect sizes [(9), but see (45,46)]. This pattern is consistent with evidence from other sensory and cognitive paradigms in ScZ (8), suggesting that neural circuits involved in the generation of high-frequency oscillations are impaired.

So far, however, studies have focused almost exclusively on the analysis of sensor-level data and source localization of auditory regions as the origin of 40-Hz ASSRs deficits. Accordingly, it is unclear which areas are fundamentally implicated beyond the auditory cortex given the contribution of extensive cortical and subcortical regions toward the generation of 40-Hz ASSRs (12,18). Koshiyama *et al.* (47) applied a Granger causality analysis, a functional connectivity measure, to assess the propagation of 40-Hz ASSRs across cortical sources in a large sample of patients with ScZ and control participants. Patients with ScZ showed a complex pattern of increased and decreased connectivity across the early transient as well as during the later sustained responses that involved temporal and frontal brain regions.

In patients with ScZ, there is evidence for a reduction in both the early transient and sustained 40-Hz ASSRs (48) that may, however, differ across early versus later illness stages (49). In addition, Kwon *et al.* (5) reported a delay between click onset and the subsequent negative peak in band-filtered time domain EEG data. This finding was replicated by Roach *et al.* (50) [see also (51)], highlighting that the phase delay deficit in patients with ScZ was associated with a significantly larger effect size than both spectral power and ITPC reductions.

An important aspect concerns the specificity of ASSR deficits toward 40-Hz stimulation. While auditory cortices during normal brain functioning respond preferentially to 40-Hz ASSRs (18), there is consistent evidence that impairments in ScZ extend to other frequencies. Thus, ASSR deficits have also been observed at 80 Hz but not at 20 or 30 Hz (52). In addition, several studies have shown that ASSRs at both delta (1–4 Hz) (53) and theta (4–7 Hz) (54) bands are reduced in ScZ as well. During normal brain functioning, there is evidence that low- and high-frequency oscillations interact: for example, the amplitude of gamma-band activity can be modulated by the phase of low-frequency (delta/theta-band) oscillations (55). However, studies that investigated cross-frequency coupling showed that 40-Hz ASSR deficits were not related to lower frequencies in ScZ (56,57).

Among the clinical correlates, correlations between increased 40-Hz ASSRs and elevated positive symptoms, especially auditory hallucinations (58,59), have been reported, which, however, has not been confirmed by other studies (52). In addition, Ogyu *et al.* (60) examined whether 40-Hz ASSRs differentiated patients with ScZ who did not respond to standard antipsychotics (treatment-resistant schizophrenia [TRS]) versus a non-TRS group. Evoked power during 40-Hz ASSRs was only impaired in the TRS group compared with the control group. However, no differences were found between TRS and non-TRS patients in 40-Hz ASSR power.

Given that gamma-band oscillations have been proposed to underlie impaired cognitive and sensory processes in ScZ (8), correlations between deficits in 40-Hz ASSRs, cognition, and possibly also functional impairments can be expected. Robust relationships with cognitive deficits have not been demonstrated so far (12,56,61). With regard to functional impairments, there is preliminary evidence that reduced 40-Hz ASSRs correlate with lower functional status in patients with ScZ (61).

Finally, several studies have examined the relationship between anatomical alterations, especially gray matter volume, and 40-Hz ASSRs in ScZ. Thus, there is evidence that gray matter reductions in the auditory cortex correlate with decreased 40-Hz ASSRs (62). A study by Du *et al.* (63) that linked resting-state functional magnetic resonance imaging data to sensor-level 40-Hz ASSRs suggested, however, that a network of brain areas consisting of the temporal medial prefrontal cortex and postcentral/precentral gyrus is associated with deficient 40-Hz ASSRs.

40-HZ ASSR DEFICITS IN EARLY-STAGE PSYCHOSIS

More recent work has investigated whether 40-Hz ASSR impairments are present during early-stage psychosis to address the potential as a biomarker for early detection and diagnosis (Table 1). This is particularly important, as early intervention can modify the trajectory of patients with FEP (64), and there is an urgent need for biomarkers to stratify patients according to clinical outcomes and pathophysiological mechanisms (65).

Currently, several studies have investigated 40-Hz ASSRs in patients with FEP (12,13,49,58,66–68), the majority of which reported robust impairments in both spectral power and ITPC, while Bartolomeo *et al.* (68) and Coffman (58) found intact 40-Hz power. With regard to CHR-P participants, Lepock *et al.* (69) showed intact ITPC and 40-Hz ASSR power, while Grent-'t-Jong *et al.* (12), Koshiyama *et al.* (66), and Tada *et al.* (49) found evidence for impaired 40-Hz ASSRs.

Furthermore, Grent-'t-Jong *et al.* (12) examined the question of whether 40-Hz ASSRs could constitute a biomarker for clinical outcomes in CHR-P participants, such as persistence of attenuated psychotic symptoms and transition to psychosis (Figure 3). Source-reconstructed 40-Hz ASSRs revealed that both the CHR-P and FEP groups had an overlapping deficit in spectral power and ITPC in the auditory cortex, hippocampus, and thalamus. Importantly, both attenuated psychotic symptom persistence and transition to psychosis were predicted by 40-Hz ASSR deficits in the hippocampus, thalamus, and superior temporal gyrus.

Several studies also examined associations between 40-Hz ASSRs, functioning, and symptoms in early-stage psychosis. Similar to findings in established ScZ, however, correlations with functioning (12,70), symptoms (12,58), and cognitive impairments (12) were inconsistent across studies.

40-HZ ASSRs, GENETICS, AND BRAIN DEVELOPMENT

The heritability of ScZ is estimated at approximately 80% (71), and recent genome-wide association studies have identified risk genes that impact on E/I balance parameters (72). There is

Table 1. 40-Hz ASSR Studies in Participants With FEP and Participants at CHR for Psychosis

Study	Clinical Group	Age, Mean (SD)	Recording Technique	Stimulus Type	Main Results ^a
Ahmed <i>et al.</i> (70)	35 CHR-P	21 (3.4)	32-channel EEG	Click trains 40 Hz	–
Spencer <i>et al.</i> (13)	34 HC	28 (8.7)	60-channel EEG	Click trains 20, 30, and 40 Hz 500-ms duration	FEP-SZ < HC: power and ITPC
	16 FE-SZ	26 (8.1)			FE-AF < HC: power and ITPC
	16 FE-AF	24 (7.4)			
Tada <i>et al.</i> (49)	21 HC	22 (3.3)	64-channel EEG	Click trains 20, 30, and 40 Hz 500-ms duration	CHR-P < HC: only late-latency power and ITPC
	15 CHR-P	22 (4.0)			FEP < HC: early-latency + late-latency power and ITPC
	13 FEP	25 (5.9)			
Koshiyama <i>et al.</i> (66)	24 HC	22 (3.0)	64-channel EEG	Click trains 20, 30, and 40 Hz 500-ms duration	CHR-P < HC: only late-latency power and ITPC
	27 CHR-P	21 (3.9)			ROSZ < HC: early-latency + late-latency power and ITPC
	21 ROSZ	24 (6.7)			
Wang <i>et al.</i> (67)	28 HC	26 (5.5)	64-channel EEG	Click trains 40 Hz 500-ms duration	FEP < HC: power and ITPC
	33 FEP	25 (6.6)			
Bartolomeo <i>et al.</i> (68)	19 HC	22 (4.3)	28-channel EEG	Click trains 40 Hz 500-ms duration	FEP = HC: power
	34 FEP	23 (3.6)			
Lepock <i>et al.</i> (69)	22 HC	22 (3.0)	32-channel EEG	Click trains 40 Hz 500-ms duration	CHR-P = HC: power and PLF
	36 CHR-P	21 (3.4)			
Grent-'t-Jong <i>et al.</i> (12)	49 HC	23 (3.6)	248-channel MEG	AM sounds 40 Hz 2000-ms duration	CHR-P < HC: ITPC in RHES, power in RTHA and RHIP
	38 CHR-N	23 (4.7)			FEP < HC: power in RHES, RTHA, and RHIP
	116 CHR-P	22 (4.5)			
	33 FEP	24 (4.5)			
Coffman <i>et al.</i> (58)	32 HC	24 (5.5)	63-channel EEG	Click trains 40 Hz 500-ms duration	FEP = HC: power and ITPC
	25 FEP	24 (4.0)			

AM, amplitude modulated; ASSR, auditory steady-state response; CHR-P, clinical high risk for psychosis; CHR-N, negative clinical high risk; EEG, electroencephalography; FEP, first-episode psychosis; FE-AF, first-episode affective disorder; FE-SZ, first-episode schizophrenia; HC, healthy control; ITPC, intertrial phase coherence; MEG, magnetoencephalography; PLF, phase-locking factor; RHES, right Heschl's gyrus; RHIP, right hippocampus; ROSZ, recent-onset schizophrenia; RTHA, right thalamus; UHR, ultra high risk.

^aIf more stimulation frequencies were presented, only the results from the 40-Hz stimulation condition are reported here.

preliminary evidence that unaffected first-degree relatives exhibit reductions in 40-Hz ASSRs (73). Moreover, computational modeling has shown the impact of common variants on 40-Hz ASSRs (74), suggesting that 40-Hz ASSR deficits are closely linked to genetic risk and therefore could constitute an endophenotype. This possibility is consistent with data showing that 40-Hz ASSR deficits can also be found in conditions that are characterized by overlapping circuit dysfunctions and genetics, such as bipolar disorder and autism spectrum disorder (75–78).

More recent studies have examined the relationship between 40-Hz ASSR deficits in 22q11.2 deletion syndrome (17,79), which is a neurogenetic disorder that confers a 30% to 40% lifetime risk for the development of psychosis (80). Several genes within the 22q11.2 region have been linked to glutamatergic and GABAergic neurotransmission (81) and disrupted migration and placement of cortical interneurons (82). Mancini *et al.* (17) examined 40-Hz ASSRs in EEG data in a sample of 22q11.2 deletion carriers and control participants (Figure 4). Both the power and ITPC of 40-Hz ASSRs as well as the evoked theta-band power were impaired in deletion carriers. Gamma-band spectral power reductions were particularly prominent in the anterior cingulate cortex, posterior cingulate

cortex, thalamus, and right primary auditory cortex. Moreover, 40-Hz ASSR deficits were pronounced in deletion carriers with psychotic symptoms and correlated with the reduction of gray matter in the auditory cortex. Importantly, a linear increase of 40-Hz ASSR spectral power was observed from childhood to adulthood in healthy control participants but not in deletion carriers.

There is converging evidence that E/I balance, such as PV+ interneurons and their excitatory inputs (83), as well as GABAergic subunits (84), undergo important modifications during adolescence, which could in turn provide not only sensitive periods for risk factors, such as cannabis (85), but also interventions that could potentially modify and even restore existing circuit dysfunctions. A study by Mukherjee *et al.* (86) examined the possibility to modify PV+ interneuron functioning in a mouse model of 22q11.2 deletion syndrome during development. Adult mice were characterized by low PV+ interneuron plasticity as well as by pronounced deficits in cognitive tasks and gamma-band oscillations. Importantly, cognitive dysfunction could be prevented permanently by dopaminergic D₂ receptor antagonist treatment or by chemogenetic activation of PV+ interneurons during late adolescence.

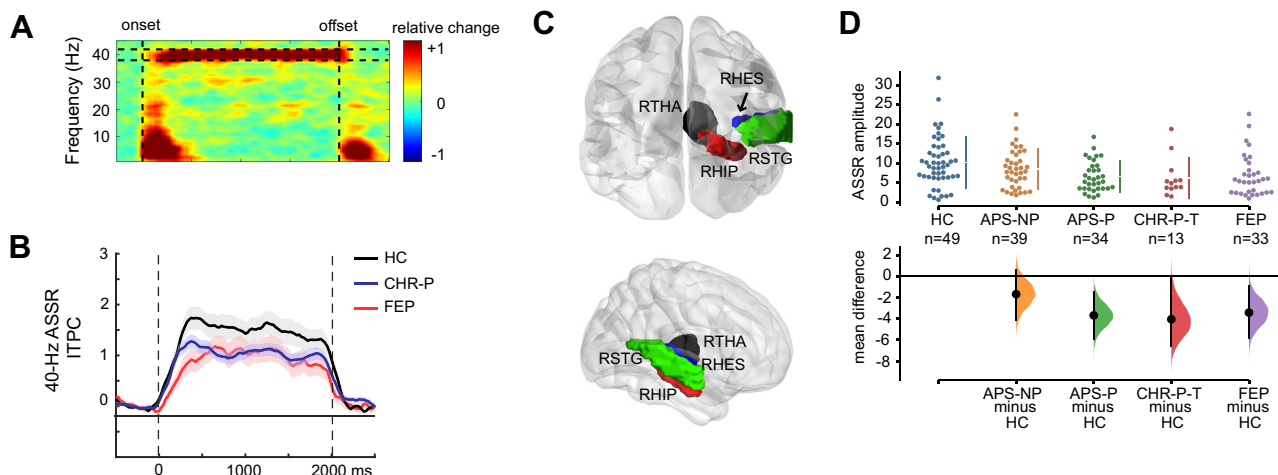


Figure 3. Clinical outcomes and 40-Hz auditory steady-state responses in early-stage psychosis. Overview of magnetoencephalography-recorded 40-Hz auditory steady-state response impairments in first-episode psychosis (FEP) patients and individuals at clinical high risk for psychosis (CHR-P). **(A)** Source-reconstructed intertrial phase coherence (ITPC) activity in the right Heschl's gyrus (RHES) for healthy control (HC) participants (top time–frequency plot). **(B)** The 40-Hz ITPC traces for the RHES in the HC (black), CHR-P (blue), and FEP (red) groups. **(C)** Regions of interest for which virtual channel data were computed and statistically examined for group differences. **(D)** Cumming estimation plots with data distribution swarm plots and group difference data, including HC participants and patients with FEP and three subgroups of CHR-P participants, based on 1-year follow-up data: nonpersistent (remitted) attenuated psychotic symptoms (APS-NP), persistent APS (APS-P) CHR-P participants who transitioned during follow-up time (CHR-P-T) (up to 36 months). Linear discriminant analysis predicting clinical outcomes of CHR-P individuals based on magnetoencephalography data for APS-P vs. APS-NP: for the right hippocampus (RHIP), right middle temporal gyrus, and right superior temporal gyrus (RSTG) ITPC, area under the curve = 0.845. A cross-validated total of 27 (69.2%) of 39 APS-NP and 25 (73.5%) of 34 APS-P participants were correctly classified. Classification of CHR-P-T vs. nontransitioned CHR-P participants: for the right thalamus (RTHA), area under the curve = 0.695. Cross-validated totals of 52 (53.6%) of 97 in the nontransitioned CHR-P group and 10 (76.9%) of 13 in the CHR-P-T group were correctly classified. These plots show the predictive value of 40-Hz auditory steady-state responses in CHR-P individuals. [Adapted with permission from Grent-’t-Jong *et al.* (12).]

40-HZ ASSR DEFICITS IN ScZ: LINK TO E/I BALANCE CIRCUIT DYSFUNCTIONS

Impaired gamma-band oscillations in ScZ have been linked to altered E/I balance parameters, in particular PV+ interneuron deficits (87) as well as NMDAR hypofunctioning (88). However, the precise pattern and contributions of NMDARs and GABAergic interneurons toward impaired gamma-band oscillations in ScZ remain unclear. One possibility is that circuit deficits are due to a primary dysfunction in inhibitory interneurons in ScZ (87). In addition, evidence exists that impaired inhibition could be the result of NMDAR hypofunctioning on PV+ interneurons (89) or reduced NMDAR drive on pyramidal cells (90).

A shift toward increased excitation as a result of NMDAR hypofunctioning has been implicated in circuit dysfunctions in ScZ, in particular during early-stage psychosis (91). Ketamine, an NMDAR antagonist, is associated with disinhibition in local (92) and large-scale networks (90) and with a dysregulation of gamma-band oscillations (93). Specifically, lower dosages of NMDAR antagonists, which elicit psychomimetic effects in healthy volunteers, cause preferentially an upregulation of both 40-Hz ASSRs (40,42) and spontaneous gamma-band oscillations (93,94). However, this pattern is not consistent with the 40-Hz ASSR findings in both CHR-P/FEP and patients with ScZ (9,10).

Increased, non-phase-locked or induced gamma-band power consistent with the NMDAR hypofunctioning model has been shown to correlate with 40-Hz ASSR ITPC deficits in ScZ (95). However, several studies that examined baseline activity during visual processing (12,96) could not confirm that

spontaneous gamma-band activity is increased. Accordingly, further studies are required to examine the significance of elevated spontaneous gamma-band activity and its relationship with stimulus-related oscillatory activity in ScZ.

Computational models have shown that decreased PV+ interneuron mediated inhibition as a result of either reduced expression of GAD67 (glutamic acid decarboxylase isoform 67 kDa) or a reduction of PV+ interneuron cell density leads to reduced 40-Hz ASSRs (36,37), with PV+ basket cells being primarily responsible for the 40-Hz ASSR results as opposed to other PV+ interneuron subclasses such as chandelier cells (97). This reduction is a result of the weakened control of the inhibitory cells over the firing of the pyramidal cell population, leading to reduced 40-Hz rhythms. In contrast, hypofunction of NMDARs on PV+ interneurons is associated with a decreased excitability in inhibitory cells (39), which decreased their recruitment during 40-Hz oscillations and, therefore, results in a reduction of 40-Hz ASSR power (38,97,98). Overall, it is conceivable that 40-Hz ASSR deficits may result from a combination of several changes to excitatory and GABAergic neurotransmission in ScZ (37).

Adams *et al.* (99) applied dynamic causal modeling to identify the contribution of diminished synaptic gain on pyramidal cells versus diminished synaptic gain on interneurons toward circuit dysfunctions in ScZ. EEG data during 40-Hz ASSRs, resting-state activity, and a mismatch negativity paradigm were analyzed and a canonical microcircuit neural mass model was employed. The results strongly favored reduced synaptic gain on pyramidal cells, which is consistent

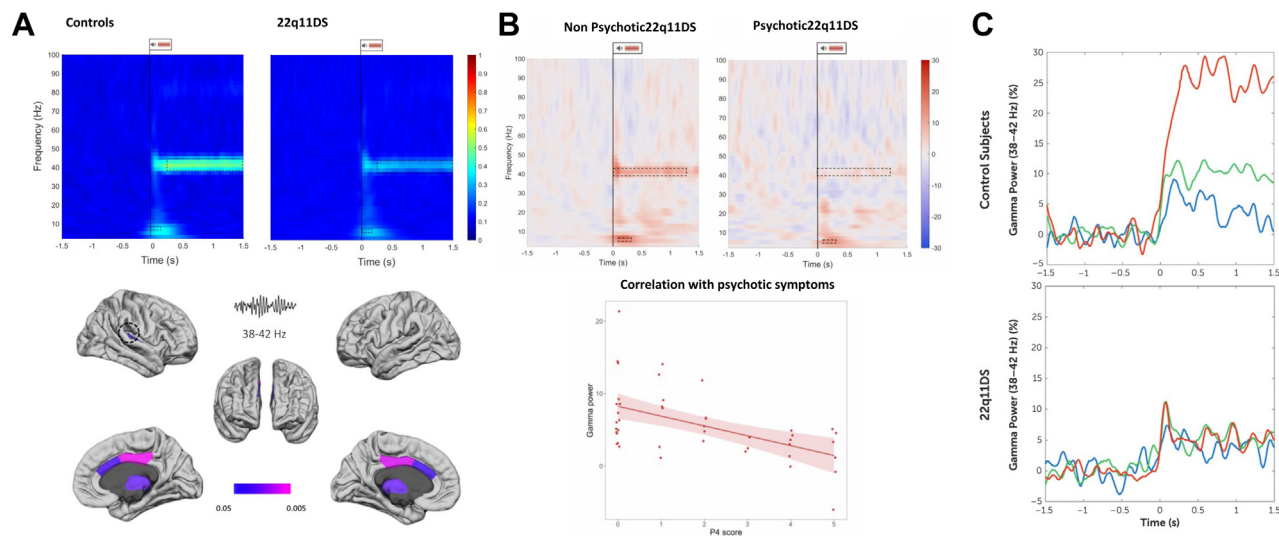


Figure 4. 40-Hz auditory steady-state responses (ASSRs) in 22q11.2 deletion syndrome (22q11DS). **(A)** Intertrial phase coherence (ITPC) values in electroencephalography data from control participants ($n = 48$) and 22q11.2 deletion carriers ($n = 58$). The outlined dotted boxes highlight the time window of statistically significant group differences in gamma-band ITPC obtained from frontocentral electrodes. (Top panel) Power values are expressed as percentages. (Bottom panel) Regions in the source space (left and right anterior cingulate cortex and superior frontal gyrus, right auditory cortex) with statistically significant lower gamma-band response (38–42 Hz) in deletion carriers ($n = 58$) compared with healthy control participants ($n = 48$) during the first 1.5 seconds of the 40-Hz ASSR. **(B)** Differences in ITPC between 22q11.2 deletion carriers with and without psychotic symptoms as defined by a score of 3 or more on the positive scale of the Structured Interview for Prodromal Syndromes. (Top panel) The deletion group with psychotic symptoms was characterized by a statistically significant reduction in 40-Hz ASSR ITPC over the entire stimulation period. (Bottom panel) Correlations between gamma-band power over frontal electrodes and scores on item P4 (perceptual abnormalities/hallucinations) from the Structured Interview for Prodromal Syndromes (hallucinations). Power values are expressed as percentages. **(C)** 40-Hz ASSR spectral power during development (childhood, adolescence, and adulthood) in control participants (top) and 22q11.2 deletion carriers (bottom). Spectral power was averaged across frontocentral electrodes, and power values are expressed in percentages. In control participants, there was a significant increase in 38- to 42-Hz power during adolescence and adulthood that was absent in the 22q11.2 deletion group. [Adapted from Mancini *et al.* (17).]

with recent postmortem data (100) that have indicated that reductions in PV+ interneurons may constitute an adaptive response to decreased excitatory drive.

Thus, the current findings suggest that 40-Hz ASSR deficits in ScZ may be compatible with altered E/I balance parameters. Specifically, evidence from pharmacology, postmortem studies, and computational modeling converges on the notion that reduced 40-Hz ASSRs in ScZ could be the result of impaired PV+ interneuron functioning (44,97). However, it is currently unclear whether this dysfunction is primary or secondary to an excitatory deficit.

While the concept of E/I imbalance has been useful to gain a first mechanistic understanding of circuit deficits in ScZ, current models of E/I balance should be extended to capture important aspects of the ASSR response and generation. For example, most models do not capture the diversity of cortical interneurons, with some exceptions (97,101). Furthermore, modeling studies so far have assumed that the ASSR response can be considered a simple summation of event-related potentials and have not addressed the entrainment of ongoing intrinsic oscillations by periodic ASSR stimuli.

RECOMMENDATIONS FOR FUTURE RESEARCH

First, it has been found that 40-Hz ASSRs are influenced by a number of experimental parameters that require careful consideration. Attention has been shown to modulate 40-Hz

ASSR power in healthy control participants (102) but not in patients with FEP (58) or in patients with ScZ (103). Accordingly, future studies need to examine and control more carefully differences in attention as a possible confound for 40-Hz ASSR deficits in ScZ.

Second, state-dependent variables, such as arousal, may impact the strength of 40-Hz ASSRs (104). This is supported by findings indicating that eyes-open versus eyes-closed conditions modulate the strength of 40-Hz ASSRs (105). It is currently unclear, however, whether these manipulations differ in ScZ or FEP groups (67,106). Finally, it has been argued that amplitude-modulated sounds, compared with click trains, are more powerful in detecting late sustained 40-Hz impairments, whereas click trains are most sensitive to detecting early-latency deficits (107). However, studies using click-train paradigms have shown sustained impairments for the duration of stimulation (9).

Regarding EEG/MEG analytic approaches, the consideration of baseline differences deserves careful consideration. Kim *et al.* (46) showed that 40-Hz ASSR impairments in patients with ScZ could only be found when the data were not baseline normalized, suggesting that higher noise levels may be present. In addition, the involvement of brain regions beyond the auditory cortex, such as the thalamus, hippocampus, and frontal regions, is not reflected in the large majority of current EEG/MEG studies. Given the extensive contribution of extended cortical and subcortical networks

toward the generation of 40-Hz ASSRs (12,18,108), future analytic protocols should ideally apply whole-brain source-localization approaches. A recent study by Grent-'t-Jong *et al.* (12), for example, showed that specifically subcortical generators in the thalamus and hippocampus were strongly impaired in CHR-P and FEP groups and that reduced 40-Hz ASSRs in the thalamus predicted transition to psychosis in CHR-P participants.

Finally, given that 40-Hz ASSRs reflect E/I balance parameters and that deficits in ITPC and spectral power may constitute a transdiagnostic biomarker, future studies could examine 40-Hz ASSRs across ScZ, bipolar disorder, and autism spectrum disorder to define potentially novel illness subtypes (109) involving E/I balance parameters.

SUMMARY

The available evidence suggests that 40-Hz ASSRs are a promising biomarker, which is robustly impaired in patients with ScZ across different paradigms and recording modalities (9,10). In addition, test-retest reliability has been established in several studies (110,111). Importantly, there is also emerging evidence that both CHR-P and FEP groups are characterized by similar impairments in ITPC and spectral power during 40-Hz stimulation (12,49) that could be potentially relevant for early detection and diagnosis. Developmental data furthermore indicate that 40-Hz ASSRs and the underlying generating mechanisms undergo major modifications during adolescence (17,83,84), indicating a sensitive period not only for risk factors, but also for intervention to correct circuit anomalies.

Moreover, the 40-Hz ASSR also fulfills the criteria for a translational and mechanistic biomarker. Data from animal work have shown that similar to findings obtained from EEG and MEG recordings in humans, 40-Hz ASSRs elicit similar perturbations in both spectral power and ITPC that can be linked to circuit mechanisms fundamentally implicated in ScZ, in particular GABAergic interneurons and NMDARs. Together with computational modeling (97,99), these data allow the testing of mechanistic hypotheses that could lead to the development of targeted and more effective interventions.

ACKNOWLEDGMENTS AND DISCLOSURES

This work was supported by the Medical Research Council (Grant No. MR/L011689/1 [to PJU]), ERA-NET (Grant No. 01EW2007A [to PJU]), Einstein Stiftung Berlin (Grant No. A-2020-613 [to PJU and CM]), and Deutsche Forschungsgemeinschaft (Grant No. UH 208/4-1 [to PJU and MB]).

PJU has received research support from Lilly and Lundbeck outside the submitted work. All other authors report no biomedical financial interests or potential conflicts of interest.

ARTICLE INFORMATION

From the Department of Child and Adolescent Psychiatry, Charité – Universitätsmedizin Berlin, corporate member of Freie Universität Berlin and Humboldt-Universität zu Berlin, Berlin, Germany (TG, MB, CM, PJU); Neural Information Processing Group, Institute of Software Engineering and Theoretical Computer Science, Technische Universität Berlin, Berlin, Germany (CM); School of Physics, Engineering and Computer Science, University of Hertfordshire, Hatfield, United Kingdom (CM); and the Institute of Neuroscience and Psychology, University of Glasgow, Glasgow, United Kingdom (PJU).

Address correspondence to Peter J. Uhlhaas, Ph.D., at peter.uhlhaas@charite.de.

Received Feb 15, 2023; revised Mar 21, 2023; accepted Mar 30, 2023.

REFERENCES

- Kraguljac NV, McDonald WM, Widge AS, Rodriguez CI, Tohen M, Nemeroff CB (2021): Neuroimaging biomarkers in schizophrenia. *Am J Psychiatry* 178:509–521.
- Wang B, Zartaloudi E, Linden JF, Bramon E (2022): Neurophysiology in psychosis: The quest for disease biomarkers. *Transl Psychiatry* 12:100.
- Picton TW, John MS, Dimitrijevic A, Purcell D (2003): Human auditory steady-state responses. *Int J Audiol* 42:177–219.
- Herrmann CS (2001): Human EEG responses to 1–100 Hz flicker: Resonance phenomena in visual cortex and their potential correlation to cognitive phenomena. *Exp Brain Res* 137:346–353.
- Kwon JS, O'Donnell BF, Wallenstein GV, Greene RW, Hirayasu Y, Nestor PG, *et al.* (1999): Gamma frequency-range abnormalities to auditory stimulation in schizophrenia. *Arch Gen Psychiatry* 56:1001–1005.
- Uhlhaas PJ, Singer W (2010): Abnormal neural oscillations and synchrony in schizophrenia. *Nat Rev Neurosci* 11:100–113.
- Singer W, Gray CM (1995): Visual feature integration and the temporal correlation hypothesis. *Annu Rev Neurosci* 18:555–586.
- Uhlhaas PJ, Singer W (2015): Oscillations and neuronal dynamics in schizophrenia: The search for basic symptoms and translational opportunities. *Biol Psychiatry* 77:1001–1009.
- Thune H, Recasens M, Uhlhaas PJ (2016): The 40-Hz auditory steady-state response in patients with schizophrenia: A meta-analysis. *JAMA Psychiatry* 73:1145–1153.
- Onitsuka T, Tsuchimoto R, Oribe N, Spencer KM, Hirano Y (2022): Neuronal imbalance of excitation and inhibition in schizophrenia: A scoping review of gamma-band ASSR findings. *Psychiatry Clin Neurosci* 76:610–619.
- Tada M, Kirihara K, Koshiyama D, Fujioka M, Usui K, Uka T, *et al.* (2020): Gamma-band auditory steady-state response as a neurophysiological marker for excitation and inhibition balance: A review for understanding schizophrenia and other neuropsychiatric disorders. *Clin EEG Neurosci* 51:234–243.
- Grent-'t-Jong T, Gajwani R, Gross J, Gumley AI, Krishnadas R, Lawrie SM, *et al.* (2021): 40-Hz auditory steady-state responses characterize circuit dysfunctions and predict clinical outcomes in clinical high-risk for psychosis participants: A magnetoencephalography study. *Biol Psychiatry* 90:419–429.
- Spencer KM, Salisbury DF, Shenton ME, McCarley RW (2008): Gamma-band auditory steady-state responses are impaired in first episode psychosis. *Biol Psychiatry* 64:369–375.
- Farahani ED, Wouters J, van Wieringen A (2021): Brain mapping of auditory steady-state responses: A broad view of cortical and subcortical sources. *Hum Brain Mapp* 42:780–796.
- Herdman AT, Wollbrink A, Chau W, Ishii R, Ross B, Pantev C (2003): Determination of activation areas in the human auditory cortex by means of synthetic aperture magnetometry. *Neuroimage* 20:995–1005.
- Koshiyama D, Miyakoshi M, Joshi YB, Nakanishi M, Tanaka-Koshiyama K, Sprock J, *et al.* (2021): Source decomposition of the frontocentral auditory steady-state gamma band response in schizophrenia patients and healthy subjects. *Psychiatry Clin Neurosci* 75:172–179.
- Mancini V, Rochas V, Seeber M, Roehri N, Rihs TA, Ferat V, *et al.* (2022): Aberrant developmental patterns of gamma-band response and long-range communication disruption in youths with 22q11.2 deletion syndrome. *Am J Psychiatry* 179:204–215.
- Tada M, Kirihara K, Ishishita Y, Takasago M, Kunii N, Uka T, *et al.* (2021): Global and parallel cortical processing based on auditory gamma oscillatory responses in humans. *Cereb Cortex* 31:4518–4532.
- Steinmann I, Gutschalk A (2011): Potential fMRI correlates of 40-Hz phase locking in primary auditory cortex, thalamus and midbrain. *Neuroimage* 54:495–504.

20. Delorme A, Makeig S (2004): EEGLAB: An open source toolbox for analysis of single-trial EEG dynamics including independent component analysis. *J Neurosci Methods* 134:9–21.
21. Reyes SA, Salvi RJ, Burkard RF, Coad ML, Wack DS, Galantowicz PJ, *et al.* (2004): PET imaging of the 40 Hz auditory steady state response. *Hear Res* 194:73–80.
22. Sukov W, Barth DS (2001): Cellular mechanisms of thalamically evoked gamma oscillations in auditory cortex. *J Neurophysiol* 85:1235–1245.
23. Ding N, Simon JZ (2009): Neural representations of complex temporal modulations in the human auditory cortex. *J Neurophysiol* 102:2731–2743.
24. Ozdamar O, Bohorquez J, Ray SS (2007): P(b)(P(1)) resonance at 40 Hz: effects of high stimulus rate on auditory middle latency responses (MLRs) explored using deconvolution. *Clin Neurophysiol* 118:1261–1273.
25. Presacco A, Bohorquez J, Yavuz E, Ozdamar O (2010): Auditory steady-state responses to 40-Hz click trains: Relationship to middle latency, gamma band and beta band responses studied with deconvolution. *Clin Neurophysiol* 121:1540–1550.
26. An KM, Shim JH, Kwon H, Lee YH, Yu KK, Kwon M, *et al.* (2022): Detection of the 40 Hz auditory steady-state response with optically pumped magnetometers. *Sci Rep* 12:17993.
27. Uhlhaas PJ, Singer W (2012): Neuronal dynamics and neuropsychiatric disorders: Toward a translational paradigm for dysfunctional large-scale networks. *Neuron* 75:963–980.
28. van Bree S, Alamia A, Zoefel B (2022): Oscillation or not—Why we can and need to know (commentary on Doelling and Assaneo, 2021). *Eur J Neurosci* 55:201–204.
29. Donoghue T, Haller M, Peterson EJ, Varma P, Sebastian P, Gao R, *et al.* (2020): Parameterizing neural power spectra into periodic and aperiodic components. *Nat Neurosci* 23:1655–1665.
30. Buzsaki G, Wang XJ (2012): Mechanisms of gamma oscillations. *Annu Rev Neurosci* 35:203–225.
31. Cardin JA (2016): Snapshots of the brain in action: Local circuit operations through the lens of gamma oscillations. *J Neurosci* 36:10496–10504.
32. Whittington MA, Traub RD, Jefferys JG (1995): Synchronized oscillations in interneuron networks driven by metabotropic glutamate receptor activation. *Nature* 373:612–615.
33. Wang XJ, Buzsaki G (1996): Gamma oscillation by synaptic inhibition in a hippocampal interneuronal network model. *J Neurosci* 16:6402–6413.
34. Petilla Interneuron Nomenclature Group, Ascoli GA, Alonso-Nanclares L, Anderson SA, Barrionuevo G, Benavides-Piccione R, Burkhalter A, *et al.* (2008): Petilla terminology: Nomenclature of features of GABAergic interneurons of the cerebral cortex. *Nat Rev Neurosci* 9:557–568.
35. Vierling-Claassen D, Cardin JA, Moore CI, Jones SR (2010): Computational modeling of distinct neocortical oscillations driven by cell-type selective optogenetic drive: Separable resonant circuits controlled by low-threshold spiking and fast-spiking interneurons. *Front Hum Neurosci* 4:198.
36. Vierling-Claassen D, Siekmeier P, Stufflebeam S, Kopell N (2008): Modeling GABA alterations in schizophrenia: A link between impaired inhibition and altered gamma and beta range auditory entrainment. *J Neurophysiol* 99:2656–2671.
37. Metzner C, Schweikard A, Zurovski B (2016): Multifactorial modeling of impairment of evoked gamma range oscillations in schizophrenia. *Front Comput Neurosci* 10:89.
38. Kirli KK, Ermentrout GB, Cho RY (2014): Computational study of NMDA conductance and cortical oscillations in schizophrenia. *Front Comput Neurosci* 8:133.
39. Carlen M, Meletis K, Siegle JH, Cardin JA, Futai K, Vierling-Claassen D, *et al.* (2012): A critical role for NMDA receptors in parvalbumin interneurons for gamma rhythm induction and behavior. *Mol Psychiatry* 17:537–548.
40. Plourde G, Baribeau J, Bonhomme V (1997): Ketamine increases the amplitude of the 40-Hz auditory steady-state response in humans. *Br J Anaesth* 78:524–529.
41. Wang X, Li Y, Chen J, Li Z, Li J, Qin L (2020): Aberrant auditory steady-state response of awake mice after single application of the NMDA receptor antagonist MK-801 into the medial geniculate body. *Int J Neuropsychopharmacol* 23:459–468.
42. Sivarao DV, Chen P, Senapati A, Yang Y, Fernandes A, Benitez Y, *et al.* (2016): 40 Hz auditory steady-state response is a pharmacodynamic biomarker for cortical NMDA receptors. *Neuropsychopharmacology* 41:2232–2240.
43. Vohs JL, Chambers RA, Krishnan GP, O'Donnell BF, Berg S, Morzorati SL (2010): GABAergic modulation of the 40 Hz auditory steady-state response in a rat model of schizophrenia. *Int J Neuropsychopharmacol* 13:487–497.
44. Hwang E, Brown RE, Kocsis B, Kim T, McKenna JT, McNally JM, *et al.* (2019): Optogenetic stimulation of basal forebrain parvalbumin neurons modulates the cortical topography of auditory steady-state responses. *Brain Struct Funct* 224:1505–1518.
45. Hamm JP, Gilmore CS, Clementz BA (2012): Augmented gamma band auditory steady-state responses: Support for NMDA hypofunction in schizophrenia. *Schizophr Res* 138:1–7.
46. Kim S, Jang SK, Kim DW, Shim M, Kim YW, Im CH, *et al.* (2019): Cortical volume and 40-Hz auditory-steady-state responses in patients with schizophrenia and healthy controls. *Neuroimage Clin* 22:101732.
47. Koshiyama D, Miyakoshi M, Joshi YB, Molina JL, Tanaka-Koshiyama K, Joyce S, *et al.* (2021): Neural network dynamics underlying gamma synchronization deficits in schizophrenia. *Prog Neuropsychopharmacol Biol Psychiatry* 107:110224.
48. Griskova-Bulanova I, Hubl D, van Swam C, Dierks T, Koenig T (2016): Early- and late-latency gamma auditory steady-state response in schizophrenia during closed eyes: Does hallucination status matter? *Clin Neurophysiol* 127:2214–2221.
49. Tada M, Nagai T, Kirihara K, Koike S, Suga M, Araki T, *et al.* (2016): Differential alterations of auditory gamma oscillatory responses between pre-onset high-risk individuals and first-episode schizophrenia. *Cereb Cortex* 26:1027–1035.
50. Roach BJ, Ford JM, Mathalon DH (2019): Gamma band phase delay in schizophrenia. *Biol Psychiatry Cogn Neurosci Neuroimaging* 4:131–139.
51. Roach BJ, Hirano Y, Ford JM, Spencer KM, Mathalon DH (2022): Phase delay of the 40 Hz auditory steady-state response localizes to left auditory cortex in schizophrenia. *Clin EEG Neurosci* 54:370–378.
52. Tsuchimoto R, Kanba S, Hirano S, Oribe N, Ueno T, Hirano Y, *et al.* (2011): Reduced high and low frequency gamma synchronization in patients with chronic schizophrenia. *Schizophr Res* 133:99–105.
53. Puvvada KC, Summerfelt A, Du X, Krishna N, Kochunov P, Rowland LM, *et al.* (2018): Delta vs gamma auditory steady state synchrony in schizophrenia. *Schizophr Bull* 44:378–387.
54. Hamm JP, Gilmore CS, Picchetti NA, Sponheim SR, Clementz BA (2011): Abnormalities of neuronal oscillations and temporal integration to low- and high-frequency auditory stimulation in schizophrenia. *Biol Psychiatry* 69:989–996.
55. Jensen O, Colgin LL (2007): Cross-frequency coupling between neuronal oscillations. *Trends Cogn Sci* 11:267–269.
56. Kirihara K, Rissling AJ, Swerdlow NR, Braff DL, Light GA (2012): Hierarchical organization of gamma and theta oscillatory dynamics in schizophrenia. *Biol Psychiatry* 71:873–880.
57. Murphy N, Ramakrishnan N, Walker CP, Polizzotto NR, Cho RY (2020): Intact auditory cortical cross-frequency coupling in early and chronic schizophrenia. *Front Psychiatry* 11:507.
58. Coffman BA, Ren X, Longenecker J, Torrence N, Fishel V, Seibold D, *et al.* (2022): Aberrant attentional modulation of the auditory steady state response (ASSR) is related to auditory hallucination severity in the first-episode schizophrenia-spectrum. *J Psychiatr Res* 151:188–196.
59. Spencer KM, Niznikiewicz MA, Nestor PG, Shenton ME, McCarley RW (2009): Left auditory cortex gamma synchronization and auditory hallucination symptoms in schizophrenia. *BMC Neurosci* 10:85.

Auditory 40-Hz Steady-State Responses in Schizophrenia

60. Ogyu K, Matsushita K, Honda S, Wada M, Tamura S, Takenouchi K, *et al.* (2023): Decrease in gamma-band auditory steady-state response in patients with treatment-resistant schizophrenia. *Schizophr Res* 252:129–137.
61. Koshiyama D, Miyakoshi M, Thomas ML, Joshi YB, Molina JL, Tanaka-Koshiyama K, *et al.* (2021): Unique contributions of sensory discrimination and gamma synchronization deficits to cognitive, clinical, and psychosocial functional impairments in schizophrenia. *Schizophr Res* 228:280–287.
62. Hirano Y, Oribe N, Onitsuka T, Kanba S, Nestor PG, Hosokawa T, *et al.* (2020): Auditory cortex volume and gamma oscillation abnormalities in schizophrenia. *Clin EEG Neurosci* 51:244–251.
63. Du X, Hare S, Summerfelt A, Adhikari BM, Garcia L, Marshall W, *et al.* (2023): Cortical connectomic mediations on gamma band synchronization in schizophrenia. *Transl Psychiatry* 13:13.
64. Correll CU, Galling B, Pawar A, Krivko A, Bonetto C, Ruggeri M, *et al.* (2018): Comparison of early intervention services vs treatment as usual for early-phase psychosis: A systematic review, meta-analysis, and meta-regression. *JAMA Psychiatry* 75:555–565.
65. McGorry P, Keshavan M, Goldstone S, Amminger P, Allott K, Berk M, *et al.* (2014): Biomarkers and clinical staging in psychiatry. *World Psychiatry* 13:211–223.
66. Koshiyama D, Kirihara K, Tada M, Nagai T, Fujioka M, Ichikawa E, *et al.* (2018): Electrophysiological evidence for abnormal glutamate-GABA association following psychosis onset. *Transl Psychiatry* 8:211.
67. Wang J, Tang Y, Curtin A, Chan RCK, Wang Y, Li H, *et al.* (2018): Abnormal auditory-evoked gamma band oscillations in first-episode schizophrenia during both eye open and eye close states. *Prog Neuropsychopharmacol Biol Psychiatry* 86:279–286.
68. Bartolomeo LA, Wright AM, Ma RE, Hummer TA, Francis MM, Visco AC, *et al.* (2019): Relationship of auditory electrophysiological responses to magnetic resonance spectroscopy metabolites in early phase psychosis. *Int J Psychophysiol* 145:15–22.
69. Lepock JR, Ahmed S, Mizrahi R, Gerritsen CJ, Maheandiran M, Drvaric L, *et al.* (2020): Relationships between cognitive event-related brain potential measures in patients at clinical high risk for psychosis. *Schizophr Res* 226:84–94.
70. Ahmed S, Lepock JR, Mizrahi R, Bagby RM, Gerritsen CJ, Korostil M, *et al.* (2021): Decreased gamma auditory steady-state response is associated with impaired real-world functioning in unmedicated patients at clinical high risk for psychosis. *Clin EEG Neurosci* 52:400–405.
71. Hilker R, Helenius D, Fagerlund B, Skytthe A, Christensen K, Werge TM, *et al.* (2018): Heritability of schizophrenia and schizophrenia spectrum based on the Nationwide Danish Twin Register. *Biol Psychiatry* 83:492–498.
72. Trubetskoy V, Pardini AF, Qi T, Panagiotaropoulou G, Awasthi S, Bigdeli TB, *et al.* (2022): Mapping genomic loci implicates genes and synaptic biology in schizophrenia. *Nature* 604:502–508.
73. Rass O, Forsyth JK, Krishnan GP, Hetrick WP, Klaunig MJ, Breier A, *et al.* (2012): Auditory steady state response in the schizophrenia, first-degree relatives, and schizotypal personality disorder. *Schizophr Res* 136:143–149.
74. Metzner C, Maki-Marttunen T, Karni G, McMahon-Cole H, Steuber V (2022): The effect of alterations of schizophrenia-associated genes on gamma band oscillations. *Schizophrenia (Heidelberg)* 8:46.
75. Owen MJ, O'Donovan MC (2017): Schizophrenia and the neurodevelopmental continuum: evidence from genomics. *World Psychiatry* 16:227–235.
76. Gandalf MJ, Zhang P, Hadjimichael E, Walker RL, Chen C, Liu S, *et al.* (2018): Transcriptome-wide isoform-level dysregulation in ASD, schizophrenia, and bipolar disorder. *Science* 362:eaat8127.
77. Jefsen OH, Shtyrov Y, Larsen KM, Dietz MJ (2022): The 40-Hz auditory steady-state response in bipolar disorder: A meta-analysis. *Clin Neurophysiol* 141:53–61.
78. Seymour RA, Rippon G, Gooding-Williams G, Sowman PF, Kessler K (2020): Reduced auditory steady state responses in autism spectrum disorder. *Mol Autism* 11:56.
79. Larsen KM, Pellegrino G, Birknow MR, Kjaer TN, Baare WFC, Didriksen M, *et al.* (2018): 22q11.2 deletion syndrome is associated with impaired auditory steady-state gamma response. *Schizophr Bull* 44:388–397.
80. Schneider M, Debbane M, Bassett AS, Chow EW, Fung WL, van den Bree M, *et al.* (2014): Psychiatric disorders from childhood to adulthood in 22q11.2 deletion syndrome: Results from the International Consortium on Brain and Behavior in 22q11.2 Deletion Syndrome. *Am J Psychiatry* 171:627–639.
81. Motahari Z, Moody SA, Maynard TM, LaMantia AS (2019): In the lineup: Deleted genes associated with DiGeorge/22q11.2 deletion syndrome: Are they all suspects? *J Neurodev Disord* 11:7.
82. Meehan DW, Tucker ES, Maynard TM, LaMantia AS (2012): Cxcr4 regulation of interneuron migration is disrupted in 22q11.2 deletion syndrome. *Proc Natl Acad Sci U S A* 109:18601–18606.
83. Caballero A, Flores-Barrera E, Cass DK, Tseng KY (2014): Differential regulation of parvalbumin and calretinin interneurons in the prefrontal cortex during adolescence. *Brain Struct Funct* 219:395–406.
84. Hashimoto T, Nguyen QL, Rotaru D, Keenan T, Arion D, Beneyto M, *et al.* (2009): Protracted developmental trajectories of GABAA receptor alpha1 and alpha2 subunit expression in primate prefrontal cortex. *Biol Psychiatry* 65:1015–1023.
85. Renard J, Rushlow WJ, Laviolette SR (2018): Effects of adolescent THC exposure on the prefrontal GABAergic system: Implications for schizophrenia-related psychopathology. *Front Psychiatry* 9:281.
86. Mukherjee A, Carvalho F, Elez S, Caroni P (2019): Long-lasting rescue of network and cognitive dysfunction in a genetic schizophrenia model. *Cell* 178:1387–1402.e14.
87. Curley AA, Lewis DA (2012): Cortical basket cell dysfunction in schizophrenia. *J Physiol* 590:715–724.
88. Javitt DC, Kantrowitz JT (2022): The glutamate/N-methyl-D-aspartate receptor (NMDAR) model of schizophrenia at 35: On the path from syndrome to disease. *Schizophr Res* 242:56–61.
89. Woo TU, Walsh JP, Benes FM (2004): Density of glutamic acid decarboxylase 67 messenger RNA-containing neurons that express the N-methyl-D-aspartate receptor subunit NR2A in the anterior cingulate cortex in schizophrenia and bipolar disorder. *Arch Gen Psychiatry* 61:649–657.
90. Krystal JH, Anticevic A, Yang GJ, Dragoi G, Driesen NR, Wang XJ, *et al.* (2017): Impaired tuning of neural ensembles and the pathophysiology of schizophrenia: A translational and computational neuroscience perspective. *Biol Psychiatry* 81:874–885.
91. Krystal JH, Anticevic A (2015): Toward illness phase-specific pharmacotherapy for schizophrenia. *Biol Psychiatry* 78:738–740.
92. Jackson ME, Homayoun H, Moghaddam B (2004): NMDA receptor hypofunction produces concomitant firing rate potentiation and burst activity reduction in the prefrontal cortex. *Proc Natl Acad Sci U S A* 101:8467–8472.
93. Rivolta D, Heidegger T, Scheller B, Sauer A, Schaum M, Birkner K, *et al.* (2015): Ketamine dysregulates the amplitude and connectivity of high-frequency oscillations in cortical-subcortical networks in humans: Evidence from resting-state magnetoencephalography-recordings. *Schizophr Bull* 41:1105–1114.
94. Pinault D (2008): N-methyl D-aspartate receptor antagonists ketamine and MK-801 induce wake-related aberrant gamma oscillations in the rat neocortex. *Biol Psychiatry* 63:730–735.
95. Hirano Y, Oribe N, Kanba S, Onitsuka T, Nestor PG, Spencer KM (2015): Spontaneous gamma activity in schizophrenia. *JAMA Psychiatry* 72:813–821.
96. Grutzner C, Wibrat M, Sun L, Rivolta D, Singer W, Maurer K, *et al.* (2013): Deficits in high- (>60 Hz) gamma-band oscillations during visual processing in schizophrenia. *Front Hum Neurosci* 7:88.
97. Metzner C, Zuroski B, Steuber V (2019): The role of parvalbumin-positive interneurons in auditory steady-state response deficits in schizophrenia. *Sci Rep* 9:18525.
98. Metzner C, Steuber V (2021): The beta component of gamma-band auditory steady-state responses in patients with schizophrenia. *Sci Rep* 11:20387.

99. Adams RA, Pinotsis D, Tsirlis K, Unruh L, Mahajan A, Horas AM, *et al.* (2022): Computational modeling of electroencephalography and functional magnetic resonance imaging paradigms indicates a consistent loss of pyramidal cell synaptic gain in schizophrenia. *Biol Psychiatry* 91:202–215.
100. Chung DW, Fish KN, Lewis DA (2016): Pathological basis for deficient excitatory drive to cortical parvalbumin interneurons in schizophrenia. *Am J Psychiatry* 173:1131–1139.
101. Siekmeier PJ, vanMaanen DP (2013): Development of antipsychotic medications with novel mechanisms of action based on computational modeling of hippocampal neuropathology. *PLoS One* 8:e58607.
102. Tiittinen H, Sinkkonen J, Reinikainen K, Alho K, Lavikainen J, Naatanen R (1993): Selective attention enhances the auditory 40-Hz transient response in humans. *Nature* 364:59–60.
103. Hamm JP, Bobilev AM, Hayrynen LK, Hudgens-Haney ME, Oliver WT, Parker DA, *et al.* (2015): Stimulus train duration but not attention moderates gamma-band entrainment abnormalities in schizophrenia. *Schizophr Res* 165:97–102.
104. Griskova I, Morup M, Parnas J, Ruksenas O, Arnfred SM (2007): The amplitude and phase precision of 40 Hz auditory steady-state response depend on the level of arousal. *Exp Brain Res* 183:133–138.
105. Griskova-Bulanova I, Ruksenas O, Dapsys K, Maciulis V, Arnfred SM (2011): Distraction task rather than focal attention modulates gamma activity associated with auditory steady-state responses (ASSRs). *Clin Neurophysiol* 122:1541–1548.
106. Griskova-Bulanova I, Dapsys K, Maciulis V, Arnfred SM (2013): Closed eyes condition increases auditory brain responses in schizophrenia. *Psychiatry Res* 211:183–185.
107. Griskova-Bulanova I, Dapsys K, Melynyte S, Voicikas A, Maciulis V, Andruskevicius S, *et al.* (2018): 40Hz auditory steady-state response in schizophrenia: Sensitivity to stimulation type (clicks versus flutter amplitude-modulated tones). *Neurosci Lett* 662:152–157.
108. Farahani ED, Goossens T, Wouters J, van Wieringen A (2017): Spatiotemporal reconstruction of auditory steady-state responses to acoustic amplitude modulations: Potential sources beyond the auditory pathway. *Neuroimage* 148:240–253.
109. Clementz BA, Sweeney JA, Hamm JP, Ivleva EI, Ethridge LE, Pearlson GD, *et al.* (2018): Identification of distinct psychosis biotypes using brain-based biomarkers. *Focus (Am Psychiatr Publ)* 16:225–236.
110. Tan HR, Gross J, Uhlhaas PJ (2015): MEG-measured auditory steady-state oscillations show high test-retest reliability: A sensor and source-space analysis. *Neuroimage* 122:417–426.
111. Roach BJ, D'Souza DC, Ford JM, Mathalon DH (2019): Test-retest reliability of time-frequency measures of auditory steady-state responses in patients with schizophrenia and healthy controls. *Neuroimage Clin* 23:101878.